

A Study on the Relationship of Heat Exchanger Design Parameters with Water Lily Stem Profile by Robust Statistical Method

Hung-Son Dang^{1*}, Thi-Anh-Tuyet Nguyen²

¹*Faculty of Vehicle and Energy Engineering, Ho Chi Minh City University of Technology and Education, Vietnam*

²*Department of Mechanical Engineering, Ho Chi Minh City University of Technology and Education, Vietnam*

*Corresponding author. Email: sondh1986@gmail.com

ARTICLE INFO

Received: 28/09/2023
Revised: 30/09/2023
Accepted: 03/10/2023
Published: 28/10/2023

KEYWORDS

Nenuphar;
Lily stems;
Bionic design;
Heat exchanger;
Taguchi method;
Optimization.

ABSTRACT

The study has successfully modeled and simulated a polymorphic tube based on the water lily stem using the robust statistical method and software. Taguchi analysis shows that the size factor E (Cross-section length of inner hole) with the effects values 39.89% has the most significant influence on the response temperature difference ($(\Delta t)^{\circ}\text{C}$). The size factor A (Peduncle diameter) has the most critical influence on the response pressure difference (ΔP (Pa)), with an effect value of 42.88%. The size factor C (Large inner hole diameter) with the significant effect value of 34.78% affects the response velocity difference (Δv (m/s)) the most. By ANOVA analysis, the results of response temperature difference analysis show that both the T-value and P-value of the size factor E (Cross-section length of inner hole) reach values that satisfy the setup requirements, with T-value reaching the most significant T-value 3.85 and the P-value 0.043 being smaller than the benchmark value 0.05, the final result indicated the size factor E (Cross-section length of inner hole) is the factor that has the most significant influence on the temperature difference of the model. For pressure difference, the results show that both the T-value and P-value of the size factor A (Peduncle diameter) reach values that satisfy the setup requirements, with the T-value reaching the largest T-value 12.19 and P-value 0.001 being smaller than the benchmark value of 0.05, the size factor A (Peduncle diameter) is the factor that has the most significant influence on the pressure difference of the model. For velocity difference, the results show that both the T-value and P-value of the size factor C (Large inner hole diameter) reach values that satisfy the set requirements, with the T-value reaching the largest T-value of 3.72 and the P-value 0.047 being smaller than the benchmark value 0.05, the size factor C (Large inner hole diameter) is the factor that has the most significant influence on the velocity difference of the model. Minitab software verification based on the Means graph drawn by Minitap17 software, the results show the best combination for response temperature difference is A3-B2-C1-D2-E2. Similarly, the best combination for response pressure and velocity differences is A2-B2-C3-D1-E1 and A2-B3-C2-D1-E3, respectively.

Doi: <https://doi.org/10.54644/jte.79.2023.1473>

Copyright © JTE. This is an open access article distributed under the terms and conditions of the [Creative Commons Attribution-NonCommercial 4.0 International License](https://creativecommons.org/licenses/by-nc/4.0/) which permits unrestricted use, distribution, and reproduction in any medium for non-commercial purpose, provided the original work is properly cited.

1. Introduction

The Biological Simulator opens the door to many advanced technologies and futuristic designs, inspired by biology to solve problems such as self-repair ability, corrosion resistance, water resistance, self-assembly, and exploitation of solar energy. A bit about the history of biological design, this term was probably first called by American biological physicist and scientist Otto Schmitt [1] in the 1950s. In a study of squid nerve tubes to try to make a natural neurotransmitter system replicator. Even so, clear examples of Biological Burns only really appeared in 1982. In 1997, the term "biological design" was once again popularized by scientists and especially author Janine Benyus, in a book entitled: Biomimicry: Innovation Inspired by Nature [2].

There are many studies in the world and in the works, when problems arise, many engineers have turned to unique structures of the natural world to reproduce to solve the issues. The following are some examples of studies and works with biological design applications. Maria E. Ferguson [3] researched the suit that helps people hover in the air, and the flying squirrel inspired this study. Yung-Jeh Chu and Wen-Tong Chong [4] researched and built wind turbines based on oil pod construction. This study builds wind turbine blades and considers their performance based on their dynamics computational retention (CFD). This cabin weighs only 66 pounds, making significant savings in both fuel and carbon emissions. Airbus's current cabins weigh 143 pounds. The goal is to lose 30% of the weight and achieve a complete 55% reduction [5]. A team of engineers at Mercedes-Benz Technology Center and Daimler Chrysler Research decided to develop a bionic-inspired car, looking to optimize the aerodynamic design. The biological model from which they drew their design inspiration was the Ostraci cubes [6]. Testing the model in a wind tunnel achieves a wind drag coefficient of only 0.06. The research results show that it is one of the best aerodynamic vehicles in this size category ever developed. According to Daimler, fuel consumption was reduced by 20%.

Research results on biological design are diverse, in addition, research on heat exchanger structure also receives a lot of attention. Tsai et al. [7] Investigations of the pressure drop and flow distribution in a chevron-type plate heat exchanger. Whang and Huang [8] made a review of Fractal Heat Exchangers Review of Fractal Heat Exchangers. Zhang et al. [9] studied flow boiling in a constructor tree-shaped mini-channel network. Chen et al. [10] investigated methanol steam reforming in a microreactor with the constructor tree-shaped network. Azad and Amidpour [11] analyze the economic optimization of shell and tube heat exchangers based on constructor theory. Yu et al. [12] study the hydraulic and thermal characteristics in fractal tree-like microchannels by numerical and experimental methods. Chai et al. [13] study heat transfer enhancement in microchannel heat sinks with periodic expansion–constriction cross-sections. Peng et al. [14] studied a novel wick structure of a vapor chamber based on the fractal architecture of the leaf vein. Guo et al. [15] investigating the application of multi-channel heat exchanger-reactor using arborescent distributors: A characterization study of the fluid distribution, heat exchange performance, and exothermic reaction. Staats and Brisson [16] study active heat transfer enhancement in air-cooled heat sinks using integrated centrifugal fans. Zhang et al. [17] Investigations of thermal and flow behavior of bifurcations and bends in fractal-like microchannel networks: Secondary flow and recirculation flow. Aute and Radermacher [18], Designs Using an Integrated Multi-Scale Analysis with Topology and Shape Optimization. Luo et al. [19] study heat and mass transfer characteristics of leaf-vein-inspired microchannels with wall thickening patterns. Wang et al. [20] make an experimental and numerical investigation of a fractal-tree-like heat exchanger manufactured by 3D printing. Foster et al. [21] study on fractal branch-like fractal shell-and-tube heat exchangers: A CFD study of the shell side performance. Huang et al. [22] study a numerical investigation of the fluid flow and heat transfer characteristics of the tree-shaped microchannel heat sink with variable cross-section. Akkaya [23] Investigation on flow and heat transfer of compact brazed plate heat exchanger with lung pattern. Zhu [24] studied Nature-Inspired Structures Applied in Heat Transfer Enhancement and Drag Reduction. Lilies are native to the Indian subcontinent [25]. In Vietnam, this tree species is widely distributed in all regions. Lilies are single leaves that grow spaced, the leaves are round or oval, the cover is sparse, the hairless underside is blue or dark purple, and the upper surface is smooth and shiny green. Lilies are profoundly lobed or round, with large, well-defined veins on the underside of the leaves. The water lily body has a circular outer section, inside with small tubes along the length of the body biological design is widely used in the design. Dang et al. [26] investigated the parameter's effect on thermal and fluid flow characteristics of heat exchanger design by utilizing the cross-section profile of the nenuphar peduncle

Today, large-size heat exchangers occupy a large area but heat exchange efficiency is not high. So, if an increase in cooling capacity is required means increasing the size of the device, this is not the best option. Therefore, in this research, we rely on the structure of the lily to apply biological design to figure out the most influential factors in heat exchange and fluid flow.

2. Methodology and implement

In this study, to understand the characteristics of heat transfer and flow in biological designs, water lily stems were selected. Collecting sample parameters is carried out by measuring the actual parameters of the samples and then screening and limiting the size parameters. Then, robust design analysis tools are applied in selecting samples, the number of factors as well and their levels. The parameter setting is via Taguchi's orthogonal matrix table, the input parameter setting factors are run randomly using Matlab software, the model is modeled using Autodesk inventor software and simulated using Ansys Fluent software. The post-simulation results are analyzed through the Taguchi and ANOVA methods and verified with Minitab software.

Experiment collection data: After being collected, the water lily stem with an outer diameter ranging from 11mm to 18mm will be measured, and a table of initial data will be established as described in Figures 1 and 2 below.



Figure 1. The process of collecting and measuring parameters on the size of *Nenurpha* Peduncle



Figure 2. The process of measuring parameters on the size of *Nenurpha* Peduncle

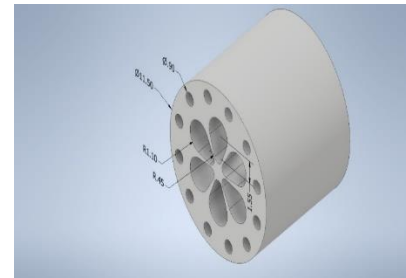


Figure 3. Building model dimension by using Autodesk Inventor 2019

Setup model parameters and their level using the robust statistical method: Selecting factors and their levels by choosing interaction elements is the most important in planning. To have a list of interactive factors that need to be investigated, in-depth knowledge of the survey problem is necessary and consultation with previous research is indispensable. The choice of level for the main factors depends on the influence of these factors on the response. If they have a linear effect, the number of levels should be 2. After analyzing the experimental data, the levels will be decided depending on the contribution percentage and error. In this study, the factors are selected based on empirical parameters measured on actual samples, in addition to previous studies conducted, the final selection result is 5 factors and the number of levels. Correspondingly for each factor are three, shown in Tables 1 and 2 below.

Orthogonal array and located data for L27 due to Taguchi method: Select the orthogonal planning table and assign the influencing factors to the orthogonal table. Before choosing an orthogonal table, it is necessary to calculate the minimum number of experiments that need to be conducted based on the total number of degrees of freedom in the survey. The minimum number of experiments must be greater than or equal to the total number of degrees of freedom, with the degree of freedom of the mean value being 1, the degree of freedom of the main factors: $n - 1$; where n is the number of levels of the element, the degree of freedom of the interaction is equal to the product of the degrees of freedom of the main factors.

Table 1. Geometrics parameters

No	Parameters (unit)	Notation	Value Range
1	Peduncle diameter (mm)	D	11.5-18
2	Outer hole diameter (mm)	d	0.9-1.1
3	Large inner hole diameter (mm)	D_{inmax}	2.2-2.5
4	Small inner hole diameter (mm)	D_{inmin}	0.9-1.1
5	Cross-section length of inner hole (mm)	L_{in}	3.1-3.4

The location of the elements in the orthogonal table is essential. In the case of multiple levels, the positions of the elements are assigned by an orthogonal table. Assigning the positions of elements in an orthogonal table can be aided by the tools of Taguchi planning. For the research to bring high accuracy and balance costs, table L27 was chosen to determine the parameters shown in Table 3.

Table 2. Parameters and values levels

Parameters Factors	Levels		
	1	2	3
A: Peduncle diameter (mm) D	11.5	15	18
B: Outer hole diameter (mm) d	0.9	1.0	1.1
C: Large inner hole diameter (mm) D_{inmax}	2.2	2.4	2.5
D: Small inner hole diameter (mm) D_{inmin}	0.9	1.0	1.1
E: Cross-section length of inner hole (mm) L_{in}	3.1	3.3	3.4

Create simulation model by Autodesk Inventor: Autodesk inventor software is used in modeling, shown in Figure 3.

Table 3. Taguchi L27 with five-factor table

Ex no.	Factors					Ex no.	Factors				
	P1	P2	P3	P4	P5		P1	P2	P3	P4	P5
1	1	1	1	1	1	15	2	2	3	2	1
2	1	1	2	2	2	16	2	3	1	1	1
3	1	1	3	3	3	17	2	3	2	2	2
4	1	2	1	2	3	18	2	3	3	3	3
5	1	2	2	3	1	19	3	1	1	3	2
6	1	2	3	1	2	20	3	1	2	1	3
7	1	3	1	3	2	21	3	1	3	2	1
8	1	3	2	1	3	22	3	2	1	1	1
9	1	3	3	2	1	23	3	2	2	2	2
10	2	1	1	2	3	24	3	2	3	3	3
11	2	1	2	3	1	25	3	3	1	2	3
12	2	1	3	1	2	26	3	3	2	3	1
13	2	2	1	3	2	27	3	3	3	1	2
14	2	2	2	1	3						

Application of MATLAB to running random distribution of input parameters for simulation

Depending on different systems, random will be designed with other algorithms, but at least need to ensure the following criteria: - The randomness of the generated results - The security of the algorithm The process of developing random numbers in the computer is called Pseudo-Random Numbers Generation (PRNG). Three typical types of randomization algorithms - Linear Congruential Generator (LCG) - Multiply with carrying (MWC) - Mersenne Twister Using a random distribution when doing the simulation helps to ensure the objectivity of the input data when we set up the simulation. The function of random distribution of simulation input parameters written on Matlab is the Function of random distribution of hot-water temperature: $85 + 2.125 * \text{randn}(1,2)$ - Function of random distribution of cold-water temperature: $25 + 0.625 * \text{randn}(1,2)$ and the function of random distribution of fluid velocity: $2.5 + 0.0625 * \text{randn}(1,2)$.

Running Simulation: There is practically no tangle-flow pattern that works well with all kinds of problems. To choose the model that best suits our needs, we need to understand the possibilities and limitations of the different options. The k-ε model is built to solve problems with fluid compression, heat exchange modeling, fluid movement, and mass transfer. The simplest turbulence models are solved by two separate equations that allow the velocity and turbulence levels to be independently determined. The standard k-ε model in Ansys Fluent has become a flow calculation model. Economically beneficial with reasonable accuracy in solving flow problems and simulating heat transfer. This is a semi-experimental model built on actual observations and combined with experience. The k-ε Standard model has its strengths and weaknesses, so some models are designed to improve its performance. Two variations are available in Ansys Fluent: RNG k-ε and Realizable k-ε. * The transport equation for the k-Standard model The turbulence kinetic energy k and its annihilation rate ε will be calculated from the following transport equations (according to equations 4.4-1, 4.4-2, Ansys manual guides, chapter 4, page 13):

$$\frac{\partial}{\partial t}(\rho k) + \frac{\partial}{\partial x_i}(\rho k u_i) = \frac{\partial}{\partial x_j} \left[\left(\mu + \frac{\mu_t}{\sigma_k} \right) \frac{\partial k}{\partial x_j} \right] + G_k + G_b - \rho \varepsilon - Y_M + S_k \quad (1)$$

And;

$$\frac{\partial}{\partial t}(\rho \varepsilon) + \frac{\partial}{\partial x_i}(\rho \varepsilon u_i) = \frac{\partial}{\partial x_j} \left[\left(\mu + \frac{\mu_t}{\sigma_\varepsilon} \right) \frac{\partial \varepsilon}{\partial x_j} \right] + C_{1\varepsilon} \frac{\varepsilon}{k} (G_k + C_{3\varepsilon} G_b) - C_{2\varepsilon} \rho \frac{\varepsilon^2}{k} + S_\varepsilon \quad (2)$$

The above two equations, which characterize the generation of kinetic energy due to velocity, which is characteristic of turbulence generation due to buoyancy, represent the contribution of the turbulent flow variation to the suppression rate. the aggregate digest is constant and tangled Prandtl numbers for k and ε, and user-defined terms.

Taguchi analysis: Analyzing experimental data is an essential step in evaluating the influence of factors on response. Analysis can be done using the ANOVA method, percentage contribution, or SN (Signal Noise) ratio. In Taguchi, the evaluation of impact criteria is based on 3 levels, average is good, more minor is better, or larger is better. Next, the SN (Signal/ Noise) Ratio will be evaluated based on the initial criteria according to the formulas. Evaluate the influence of factors:

Smaller is better

$$SN_i = -10 \log \sum_{u=1}^{N_i} \frac{\bar{y}_u^2}{N_i} \quad (3)$$

Bigger is better

$$SN_i = -10 \log \frac{1}{N_i} \sum_{u=1}^{N_i} \frac{1}{\bar{y}_u^2} \quad (4)$$

Where i: experiment number (Experiment number) u: trial number (Trial number) Ni: number of trials for experiment i (Number of trials for experiment i). After calculating the SN value, we set up a table with the SN value, calculating the average value of SN for each level. After calculating the average values of S/N, assigning the values to the table and giving the R-value (rank) after comparing the values in the table. R with value 1 is the most influential factor and vice versa, as described in table 4 below.

Table 4. Table of average values of SN ratio

No.	P1	P2	P3	P4	P5
1	SN _{P1,1}	SN _{P2,1}	SN _{P3,1}	SN _{P4,1}	SN _{P5,1}
2	SN _{P1,2}	SN _{P2,2}	SN _{P3,2}	SN _{P4,1}	SN _{P5,2}
3	SN _{P1,3}	SN _{P2,3}	SN _{P3,3}	SN _{P4,3}	SN _{P5,3}
Δ	R _{P1}	R _{P2}	R _{P3}	R _{P4}	R _{P5}
Rank

ANOVA analysis: The goal of the method is to compare the average results of many groups (overall) based on the average values of observed samples from these groups and through hypothesis testing to conclude the equality of the groups. average number. In this study, variance analysis examines the influence of one or several causal factors (qualitative) on an outcome factor (quantitative). One-factor analysis of variance is used to analyze the impact of a cause factor on an outcome factor under study. Suppose we need to compare the average of k-independent populations. We take k with observed denominators $n_1, n_2, n_3 \dots n_k$; follows a normal distribution. The standard of the populations is denoted as $\mu_1, \mu_2, \mu_3 \dots \mu_k$, the variance analysis model with one influencing factor is described in the form of hypothesis testing as follows:

$$H_0 : \mu_1 = \mu_2 = \mu_3 = \dots = \mu_k \tag{5}$$

To test, we offer three solutions: Each sample follows an average distribution N, and the overall variances are equal. We take k-independent samples from the k population. Each sample is observed n_j times. The steps include the following 4 steps:

Step 1: Calculate sample means and overall averages of k samples based on the one-factor ANOVA analysis shown in Table 5.

Step 2: Calculate the sums of squared deviations and determine the squared deviations of the groups

Step 3: Calculate the variances (intra-group variance and between-group variance) where k is the number of groups (sample) and n is the total number of observations of the groups. MSW is the within-group variance, and MSB is the between-group variance. Finally, to perform hypothesis testing, step 4 is conducted for this purpose.

Table 5. The one-factor ANOVA analysis table.

No.	k				
	1	2	3	...	K
1	X_{11}	X_{12}	X_{13}		X_{1k}
2	X_{21}	X_{22}	X_{23}		X_{2k}
...					
j	X_{j1}	X_{j2}	X_{j3}		X_{jk}
Ave	\bar{x}_1	\bar{x}_2	\bar{x}_3		\bar{x}_k

Average, $\bar{x}_1, \bar{x}_2, \bar{x}_k$ calculated by equation:

$$\bar{x}_i = \frac{\sum_{j=1}^{n_i} X_{ij}}{n_i} \quad (i = 1, 2, 3, \dots, k) \tag{6}$$

Average k calculated by equation:

$$\bar{x} = \frac{\sum_{i=1}^k n_i \bar{x}_i}{\sum_{i=1}^k n_i} \quad (i = 1, 2, 3, \dots, k) \tag{7}$$

Directional deviation group 1:

$$SS_1 = \sum_{j=1}^{n_1} (X_{j1} - \bar{x}_1)^2 \tag{8}$$

Directional deviation group k:

$$SS_k = \sum_{j=1}^{n_k} (X_{jk} - \bar{x}_k)^2 \tag{9}$$

Step 4: Test the hypothesis. Calculated according to the F test standard (experimental F). With theoretical F is the limit T-value found from the F distribution table with k-1 degrees of freedom of variance in the numerator and n-k degrees of freedom of variance in the denominator with significance

level α . Theoretical F can be looked up through the FINV function ($\alpha, k-1, n-1$) in Excel. If experimental $F >$ theoretical F, reject H_0 , meaning the population average k is unequal.

Minitab analysis: Minitab 17 is used to reprocess the data obtained from the simulation to analyze the results and verify those values after being analyzed with Taguchi and ANOVA.

3. Results and Discussion

The results of the ansys simulation: In this study, to understand the heat transfer characteristics and flow properties of the device, the results of the responses on the temperature field, pressure field, and velocity field are collected for analysis. The simulation results of these values are shown in Figures 4,5,6 and 7 below. Table 6 shows the simulation results for 27 cases, currently, the model for temperature difference across the sample ($(\Delta t) ^\circ C$) is of interest, followed by the model for pressure difference (ΔP (Pa)), and finally the model for transport difference velocity (Δv (m/s)).

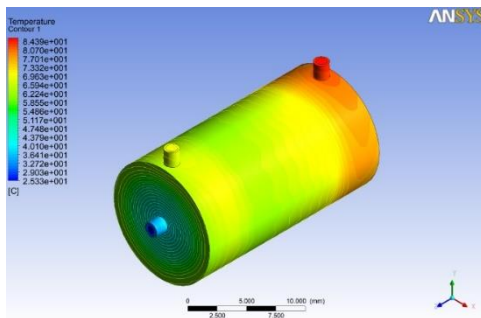


Figure 4. The contour temperature results of the model

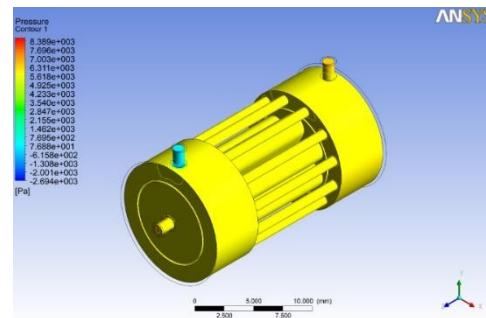


Figure 5. The contour pressure results of the model

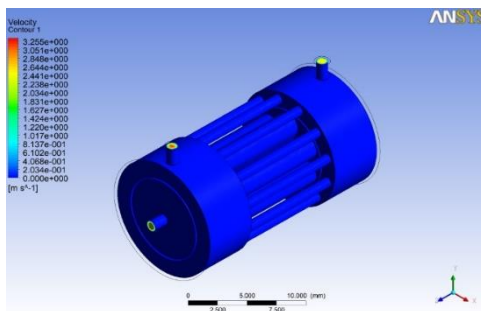


Figure 6. The contour velocity results of the model

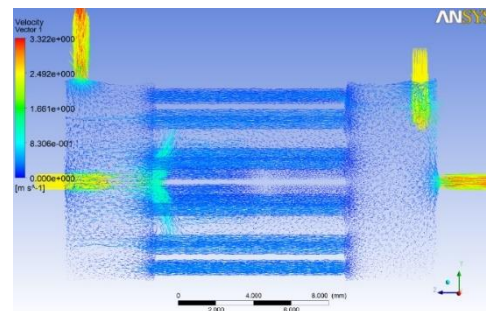


Figure 7. The vector velocity results of the model

Table 6. Table of temperature, pressure, and velocity differences after simulation.

No.	$(\Delta t) ^\circ C$	ΔP (Pa)	Δv (m/s)	No.	$(\Delta t) ^\circ C$	ΔP (Pa)	Δv (m/s)
1	60.287	11313.22	3.3225	14	64.250	9676.25	3.1193
2	57.753	11960.55	3.3499	15	57.561	10436.74	3.2898
3	59.753	11166.91	3.2461	16	62.377	10417.94	3.2643
4	55.830	13251.38	3.5184	17	54.958	11168.53	3.3651
5	62.049	11548.32	3.3439	18	56.602	10309.81	3.2621
6	59.950	11148.58	3.2851	19	60.085	9976.36	3.2796
7	55.319	12380.62	3.4014	20	60.598	11143.13	3.2975
8	60.970	9975.86	3.1851	21	60.129	9643.56	3.1821
9	58.418	11394.46	3.3457	22	57.545	10362.83	3.3607
10	61.832	11406.97	3.3903	23	59.799	9273.26	3.1718
11	57.661	11214.35	3.3467	24	59.639	11024.29	3.4532
12	62.622	10290.08	3.2203	25	58.570	10819.49	3.2478
13	55.630	10416.07	3.2853	26	59.359	10129.90	3.1753
				27	58.860	10869.05	3.2719

The results of Taguchi analysis: The simulation results are analyzed using the Taguchi method to evaluate the parameters based on the SN ratio. At first, by calculating the value of SN, table 7 shows the results of SN corresponding to each factor affecting the temperature difference ($(\Delta t)^{\circ}\text{C}$) of the sample. The calculation and analysis show that the size factor E (Cross-section length of inner hole) with the effects values 39.89% and rank 1 has the most significant influence on the temperature difference.

Then, table 8 shows the results of SN corresponding to each factor affecting the pressure difference (ΔP (Pa)) of the model. With the above calculation, the results show that the size factor A (Peduncle diameter) has the most significant influence on the pressure difference, with effect T-value and rank are 42.88% and 1, respectively.

Finally, SN analysis and the effect of parameters on model velocity difference (Δv (m/s)) was shown in Table 9.

The results show that the size factor C (Large inner hole diameter) with the significant effect T-value of 34.78% affects the velocity difference the most.

Table 7. SN analysis and effect of parameters on model temperature

	A	B	C	D	E
1	-35.4566	-35.4327	-35.4637	-35.5889	-35.4634
2	-35.4193	-35.5683	-35.5307	-35.4219	-35.3601
3	-35.515	-35.4686	-35.4752	-35.4587	-35.6461
Means	0.044313	0.057121	0.026185	0.067924	0.129785
Effects	13.62%	17.56%	8.05%	20.88%	39.89%
Rank	4	3	5	2	1

Table 8. SN analysis and effect of parameters on model pressure

	A	B	C	D	E
1	-81.2376	-80.7288	-80.8955	-80.595	-80.6037
2	-80.3522	-80.5133	-80.5606	-80.8195	-80.7006
3	-80.4094	-80.7572	-80.5432	-80.6087	-80.695
Means	0.314203	0.153103	0.123245	0.079426	0.062727
Effects	42.88%	20.90%	16.82%	10.84%	8.56%
Rank	1	2	3	4	5

Table 9. SN analysis and effect of parameters on model velocity

	A	B	C	D	E
1	-10.4606	-10.3915	-10.4805	-10.3445	-10.3818
2	-10.3323	-10.3765	-10.3065	-10.418	-10.4169
3	-10.3419	-10.3668	-10.3479	-10.3285	-10.3362
Means	0.045949	0.011441	0.071816	0.035149	0.042113
Effects	22.25%	5.54%	34.78%	17.02%	20.41%
Rank	2	5	1	4	3

The result of the ANOVA analysis: ANOVA analysis of variance was performed to compare the results with Taguchi to evaluate the independence of the two methods. Table 10 shows the results of temperature difference analysis according to ANOVA. The results show that both the T-value and P-value of the size factor E (Cross-section length of inner hole) reach values with the largest T-value of

3.85 and P-value of 0.043 being smaller than the benchmark value of 0.05, the size factor E (Cross-section length of inner hole) is the factor that has the most significant influence on the temperature difference of the sample.

Table 10. ANOVA table of parameters on model temperature difference

Source	DF	Adj SS	Adj MS	F-Value	P-Value
A	2	7.607	3.8036	1.62	0.229
B	2	4.216	2.1079	0.90	0.427
C	2	1.166	0.5832	0.25	0.783
D	2	6.920	3.4601	1.47	0.259
E	2	18.080	9.0398	3.85	0.043
Error	16	37.581	2.3488		
Total	26	75.570			

Table 11. ANOVA table of parameters on model pressure difference

Source	DF	Adj SS	Adj MS	F-Value	P-Value
A	2	7012050	3506025	12.19	0.001
B	2	523140	261570	0.91	0.423
C	2	1123500	561750	1.95	0.174
D	2	512652	256326	0.89	0.430
E	2	95003	47501	0.17	0.849
Error	16	4601903	287619		
Total	26	13868247			

Table 11 shows the results of pressure difference analysis according to ANOVA. The results show that both the T-value and P-value of the size factor A (Peduncle diameter) reach values with the largest T-value of 12.19 and the P-value 0.001 being smaller than the benchmark value 0.05, the size factor A (Peduncle diameter) is the factor that has the most significant influence on the temperature difference of the sample. Table 12 shows the results of velocity difference analysis according to ANOVA. The results show that both the T-value and P-value of the size factor C (Large inner hole diameter) reach values with the largest T-value of 3.72 and P-value 0.047 being smaller than the benchmark value of 0.05, the size factor C (Large inner hole diameter) is the factor that has the most significant influence on the temperature difference of the sample.

Table 12. ANOVA table of parameters on model velocity difference

Source	DF	Adj SS	Adj MS	F-Value	P-Value
P1	2	0.013259	0.006630	2.29	0.134
P2	2	0.000378	0.000189	0.07	0.937
P3	2	0.021598	0.010799	3.72	0.047
P4	2	0.003610	0.001805	0.62	0.549
P5	2	0.004331	0.002166	0.75	0.490
Error	16	0.046386	0.002899		
Total	26	0.089562			

The results of Minitab analysis: From ANOVA's theory about hypothesis testing, we conclude that factors affect the product. Considering the results, we going to use minitab17 to run the calculation to verify again the analysis result.

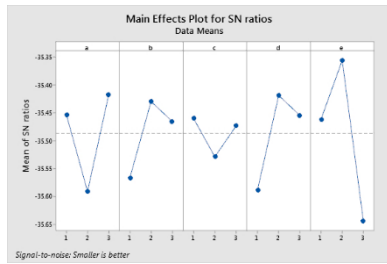


Figure 8. Main effects plot for SN ratios of model temperature difference

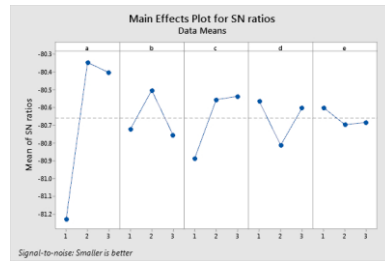


Figure 9. Main effects plot for SN ratios of model pressure difference

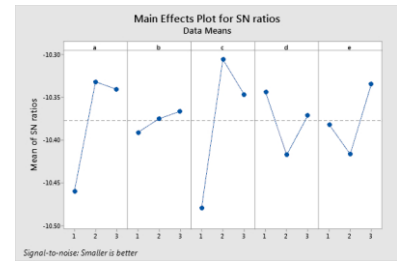


Figure 10. Main effects plot for SN ratios of model velocity difference

Figure 8 shows the main effect plot for SN ratio, based on the Means graph drawn by Minitap17 software, we choose the best combination for model temperature difference: A3-B2-C1-D2-E2. Similarly, figures 9 and 10 show the main effect plot for the SN ratio, based on the Means graph drawn by Minitap17 software for the best combination for model pressure difference and velocity difference is A2-B2-C3-D1-E1 and A2-B3-C2-D1-E3, respectively.

4. Conclusions

The study has successfully modeled and simulated a polymorphic tube based on the water lily stem using the mentioned tools and software. According to Taguchi, the calculation and analysis show that the size factor E (Cross-section length of inner hole) with the effects values 39.89% and rank 1 has the most significant influence on the response temperature difference, the size factor A (Peduncle diameter) has the most critical influence on the response pressure difference, with effect value and rank are 42.88% and 1, respectively. The size factor C (Large inner hole diameter), with a significant effect value of 34.78%, affects the response velocity difference. ANOVA, the results of temperature difference analysis according to ANOVA. The results show that both the T-value and P-value of the size factor E (Cross-section length of inner hole) reach values that satisfy the set requirements, with the T-value reaching the largest T-value 3.85 and the P-value 0.043 being smaller than the benchmark value 0.05, the size factor E (Cross-section length of inner hole) is the factor that has the most significant influence on the response temperature difference of the model. The results of pressure difference analysis according to ANOVA. It shows that both the T-value and P-value of the size factor A (Peduncle diameter) reach values that satisfy the set requirements, with the T-value reaching the largest T-value of 12.19 and the P-value 0.001 being smaller than the benchmark value of 0.05, the size factor A (Peduncle diameter) is the factor that has the most significant influence on the response pressure difference of the model. The results of velocity difference analysis according to ANOVA. It shows that both the T-value and P-value of the size factor C (Large inner hole diameter) reach values that satisfy the set requirements, with the T-value reaching the largest T-value of 3.72 and the P-value 0.047 being smaller than the benchmark value of 0.05, the size factor C (Large inner hole diameter) is the factor that has the most significant influence on the response velocity difference of the model. Minitab software verification based on the Means graph drawn by Minitap17 software, we choose the best combination for response temperature difference is A3-B2-C1-D2-E2, where the factor and their level are described in Tables 1 and 2. Similarly, figures 10 and 11 show the main effect plot for the SN ratio, based on the Means graph drawn by Minitap17 software for the best combination for response pressure difference and velocity difference is A2-B2-C3-D1-E1 and A2-B3-C2-D1-E3, respectively.

Acknowledgments

We acknowledge the support and time provided by Ho Chi Minh City University of Technology and Education (HCMUTE), as well as the use of their facilities in this study.

REFERENCES

- [1] O. H. Schmitt, "A Lifetime of Connections: Otto Herbert Schmitt, 1913-1998," *Physics in Perspective*, vol. 4, no. 4, pp. 456-490, 2002.
- [2] J. M. Benyus, *Biomimicry: Innovation Inspired by Nature*, Kindle Ed. New York, NY, USA: Harper Collins, 2009.
- [3] M. E. Ferguson, "Flying without Dying: The Future of Wingsuit Design," *Technical Writing Final Project*, Washington University in St. Louis., 2016.
- [4] Y. J. Chu and W. T. Chong, "A biomimetic wind turbine inspired by *Dryobalanops aromatica* seed," *Computers & Fluids*, vol. 159, pp. 295-315, 2017.
- [5] K. Micallef. "Airbus Continues to Innovate Bionic Design for Future Sustainable Flights." [autodesk.com. https://www.autodesk.com/design-make/articles/bionic-design](https://www.autodesk.com/design-make/articles/bionic-design) (accessed Nov. 26, 2019).
- [6] C. M. Yang, H. J. Ying, W. Y. Li, and L. Y. Hsuan, "Analysis of Mercedes-Benz Concept Car Using Biomimicry Design Spiral and Template Analysis-An Exploratory Study," *International Journal of Innovation in Management*, vol. 7, no. 2, pp. 49-56, 2019.
- [7] Y. C. Tsai, F. B. Liu, and P. T. Shen, "Investigations of the pressure drop and flow distribution in a chevron-type plate heat exchanger," *International Communications in Heat and Mass Transfer*, vol. 36, no. 6, pp. 574-578, 2009.
- [8] Y. Whang and Z. Huang, "Review of Fractal Heat Exchangers," in *International Refrigeration and Air Conditioning Conference*, 2016, Paper 1725.
- [9] C. Zhang, Y. Chen, R. Wu, and M. Shi, "Flow boiling in constructal tree-shaped minichannel network," *International Journal of Heat and Mass Transfer*, vol. 54, no. 1-3, pp. 202-209, 2011.
- [10] Y. Chen and C. Zhang, "Methanol steam reforming in microreactor with constructal tree-shaped network," *Journal of Power Sources*, vol. 196, no. 15, pp. 6366-6373, 2011.
- [11] A. V. Azad and M. Amidpour, "Economic optimization of shell and tube heat exchanger based on constructal theory," *Energy*, vol. 36, no. 2, pp. 1087-1096, Feb. 2011.
- [12] X. F. Yu, C. P. Zhang, and J. T. Teng, "A study on the hydraulic and thermal characteristics in fractal tree-like microchannels by numerical and experimental methods," *International Journal of Heat and Mass Transfer*, vol. 55, no. 25-26, pp. 7499-7507, Dec. 2012.
- [13] L. Chai, G. Xia, L. Wang, M. Zhou, and Z. Cui, "Heat transfer enhancement in microchannel heat sinks with periodic expansion-constriction cross-sections," *International Journal of Heat and Mass Transfer*, vol. 62, pp. 741-751, 2013.
- [14] Y. Peng *et al.*, "A novel wick structure of vapor chamber based on the fractal architecture of leaf vein," *International Journal of Heat and Mass Transfer*, vol. 63, pp. 120-133, Aug. 2013.
- [15] X. Guo, Y. Fan, and L. Luo, "Multi-channel heat exchanger-reactor using arborescent distributors: A characterization study of fluid distribution, heat exchange performance and exothermic reaction," *Energy*, vol. 69, pp. 728-741, May 2014.
- [16] W. L. Staats and J. G. Brisson, "Active heat transfer enhancement in air cooled heat sinks using integrated centrifugal fans," *International Journal of Heat and Mass Transfer*, vol. 82, pp. 189-205, Mar. 2015.
- [17] C. P. Zhang *et al.*, "Investigations of thermal and flow behavior of bifurcations and bends in fractal-like microchannel networks: Secondary flow and recirculation flow," *International Journal of Heat and Mass Transfer*, vol. 85, pp. 723-731, Jun. 2015.
- [18] V. Aute and R. Radermacher, "Designs Using an Integrated Multi-Scale Analysis with Topology and Shape Optimization," in *International Refrigeration and Air Conditioning Conference*, West Lafayette, IN, USA, 2016.
- [19] Y. Luo, W. Liu, L. Wang, and W. Xie, "Heat and mass transfer characteristics of leaf-vein-inspired microchannels with wall thickening patterns," *International Journal of Heat and Mass Transfer*, vol. 101, pp. 1273-1282, Oct. 2016.
- [20] G. Wang *et al.*, "Experimental and numerical investigation of fractal-tree-like heat exchanger manufactured by 3D printing," *Chemical Engineering Science*, vol. 195, pp. 250-261, Feb. 2019.
- [21] N. Foster, D. S. Saez, and H. A. Garcia, "Fractal branch-like fractal shell-and-tube heat exchangers: A CFD study of the shell side performance," *IFAC-PapersOnLine*, vol. 52, no. 1, pp. 100-105, 2019.
- [22] P. Huang, G. Dong, X. Zhong, and M. Pan, "Numerical investigation of the fluid flow and heat transfer characteristics of tree-shaped microchannel heat sink with variable cross-section," *Chemical Engineering and Processing - Process Intensification*, vol. 147, p. 107769, Jan. 2020.
- [23] V. R. Akkaya, "Investigation on flow and heat transfer of compact brazed plate heat exchanger with lung pattern," *Applied Thermal Engineering*, vol. 175, p. 115309, Jul. 2020.
- [24] Z. Zhu *et al.*, "Nature-Inspired Structures Applied in Heat Transfer Enhancement and Drag Reduction," *Micromachines (Basel)*, vol. 12, no. 6, p. 656, Jun. 2021.
- [25] G. V. D. Velde, "A project on nymphaeid-dominated systems," *Hydrobiological Bulletin*, vol. 15, pp. 185-189, 1981.
- [26] H. S. Dang, T. A. T. Nguyen, and C. H. Hsu, "Investigating the parameters effect on thermal and fluid flow characteristics of heat exchanger design by using the cross-section profile of nenuphar peduncle," in *ATE HEFAT Conference*, 2021.



Dang Hung Son received a B.S from the Faculty of Automotive and Energy Engineering, HCMC University of Technology and Education (HCMUTE), Viet Nam, in 2009 and a Master of Science, Ph.D. degree in the College of Mechanical Engineering, Chung Yuan Christian University, Zhongli, Taoyuan, Taiwan, in 2013 and 2017, respectively. Currently, he is a lecturer at the Faculty of High-Quality Training and the Faculty of Automotive and Energy Engineering, Ho Chi Minh City University of Technology and Education.



Nguyen Thi Anh Tuyet received the B.S from the Faculty of Auditing and Accounting, Ho Chi Minh Banking University, Viet Nam, in 2009 and the Master of Science, Ph.D. degree in the Department of Industrial System Engineering, Chung Yuan Christian University, Zhongli, Taoyuan, Taiwan, in 2014 and 2018, respectively. Currently, she is a lecturer at the Department of Industrial System Engineering, Faculty of Mechanical Engineering, Ho Chi Minh City University of Technology and Education. Email: ntatuyet@hcmute.edu.vn